Asphalt mixture performance and testing

# Thermomechanical behaviour of interfaces between pavement layers made in bituminous mixtures

*Thomas Attia[1], Hervé Di Benedetto[1], Cédric Sauzéat[1], Simon Pouget[2]*
*[1]University of Lyon/Ecole Nationale des Travaux Publics de l'Etat (ENTPE), [2]Eiffage Infrastructures, Research & Innovation Department*

Abstract

The strain and stress fields within the pavement depend strongly on interfaces behaviour. Therefore, the properties of interfaces between bituminous mixtures layers should be a major concern when designing pavements. The usual but inaccurate assumptions of layers being perfectly bonded or completely unbonded can lead to premature degradation of the pavement. A better knowledge of interfaces behaviour is a first step towards more efficient design methods. In this paper, the thermomechanical behaviour of different interfaces was studied using the new and innovative 2T3C Hollow Cylinder Apparatus (2T3C HCA). The samples (13 cm height, 17.2 cm external diameter and 12.2 cm internal diameter) are composed of two bituminous mixtures layers bonded at the interface with a tack coat. They can be cored in situ or from laboratory prepared slabs. Shear and tension/compression can be applied independently on the samples. Strain in the bituminous mixtures and displacement gap at the interface are obtained using 3D Digital Image Correlation. The linear viscoelastic behaviour of bituminous mixtures as well as the one of the interface could be determined. They have been studied from small strain cyclic tests at multiple frequencies and temperatures. The complex modulus of the two bituminous mixtures and the complex interface modulus are obtained in tension/compression and shear modes. The monotonic shear failure of interfaces has also been studied with different normal pressures.

This paper was first published in 2020 in version 1.0 of the proceedings of the 7th E&E Congress. This second edition (version 1.1.) of the proceedings is published in June 2021. The content of this paper has not changed, but the author(s) may have provided additional information in the form of an annex.

## 1. INTRODUCTION

Pavement design methods become more and more rational. For instance, the American design method has gone from empirical to semi-empirical with the introduction of mechanical calculations to validate the structure chosen by the designer [1]. The mechanical model used to represent the structure, the same than the one used in the French rational method [2], is an elastic multi-layer pavement. The strain and stress in the structure are found using Burmister method [3]. In this model, the layers are considered either fully bonded or fully unbonded. In most cases, interfaces between layers in bituminous mixtures are considered perfectly bonded. However, the strain field depends strongly on the interface behaviour. If the layers are bonded, then they act mechanically as one and tensile strains are only found at the bottom of the structure but if they are unbonded, high tensile strains are found at the bottom of each layer [4] which dramatically reduces the whole structure's lifetime. Taking into account a realistic behaviour of interfaces is a major way of improving design methods but it is a difficult task since the stress state at the interface is very complex [5]. The stress tensor has indeed six independent components that should all be considered to predict the interface response. In addition, the bituminous materials interacting at the level of the interface (the bituminous mixtures in the layers and the eventual tack coat usually a bituminous emulsion) show a viscoelastic behaviour depending on the temperature but also on the amplitude of loading and of the number of loading cycles [6] and one would expect that interfaces present a viscoelastic behaviour too.
Beginning in the 1970's, the testing of interfaces behaviour focused on shear bond strength evaluation in a first time. These tests were based on the observation of the slippage between layers that occurred when the bond at the interface failed, often in areas subjected to high horizontal loading due to accelerating, braking or turning vehicles. The most common test is the guillotine test first introduced by Leutner [7] which consists in applying a vertical force on the end of a bi-layered cylindrical specimen fixed horizontally. It was adapted many times afterwards [8,9], sometimes with the possibility to add a normal loading while shear is applied [10,11]. Shear box test [12] or inclined shear tests [13] were also developed to test interfaces shear bond. Yet, the stress state at the interface in shear tests is far from being representative of what happens in real pavements [5] especially because in all the previously mentioned tests the normal pressure, if it exists, is constant, dependant on the shear loading or uncontrollable. A more representative test should be able to apply a normal pressure independently of the shear loading. It should also be able to apply cyclic loading to better simulate traffic action on the pavement.
The objective of this paper is to present an advanced characterization of the thermomechanical behaviour of an interface between bituminous mixtures layers using the innovative apparatus device 2T3C Hollow Cylinder Apparatus ("*Torsion-Traction/Compression sur Cylindre Creux*", in French). This apparatus was developed at the ENTPE/University of Lyon and is able to precisely characterize the viscoelastic behaviour of interface for small strains but also to observe the shear failure behaviour.

## 2. 2T3C HOLLOW CYLINDER APPARATUS (2T3C HCA)

The 2T3C HCA can apply torsion and/or tension/compression to hollow cylinder samples. The dimensions of a sample are: an external radius of 86 mm, an internal radius of 61 mm and a height of 125 mm. The samples can be composed of two bituminous mixtures layers as presented in Figure 1 but other road materials can be tested. The sample dimensions were chosen so as to have a homogeneous stress field in the sample with a good approximation using the recommendations of Hight *et al.* [14]. The samples are made in laboratory or cored in pavements in use.

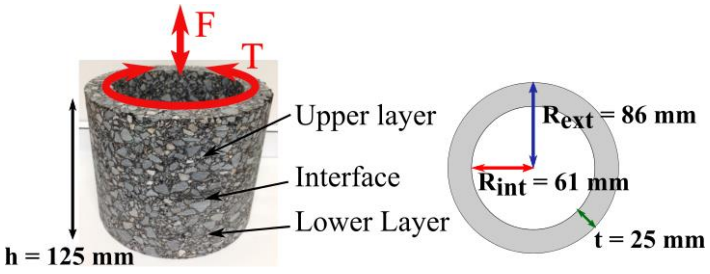


**Figure 1 – Hollow cylinder sample of the 2T3C HCA**

The torsion and the tension/compression can be applied independently to the sample thanks to a servohydraulic press having one load cell for the torque and one load cell for the axial force. Any loading path in the σ-τ plane (normal stress-shear stress) is feasible (Figure 2). Cyclic testing can be performed at a maximum frequency of 10 Hz with sinusoidal loadings or any cyclic loading. The axial force can be measured up to 100 kN (accuracy of 0.01 kN) and the torque up to 2000 N.m (accuracy of 1 N.m), which corresponds to a maximum normal stress of 8.7 MPa and a maximum shear stress of 2.3 MPa which is enough to study interface failure under common testing temperature and loading speeds. Sample temperature is controlled using a thermal chamber. PT100 sensors are placed on the inside and outside surfaces of the samples to check the homogeneity of the temperature field. Four non-contact sensors

(eddy currents sensors), one pair on each side of the sample, are used to control and measure the global displacements between the top and the bottom of the sample with a precision of 0.1 µm both in the vertical direction and in the horizontal direction related to the rotation.

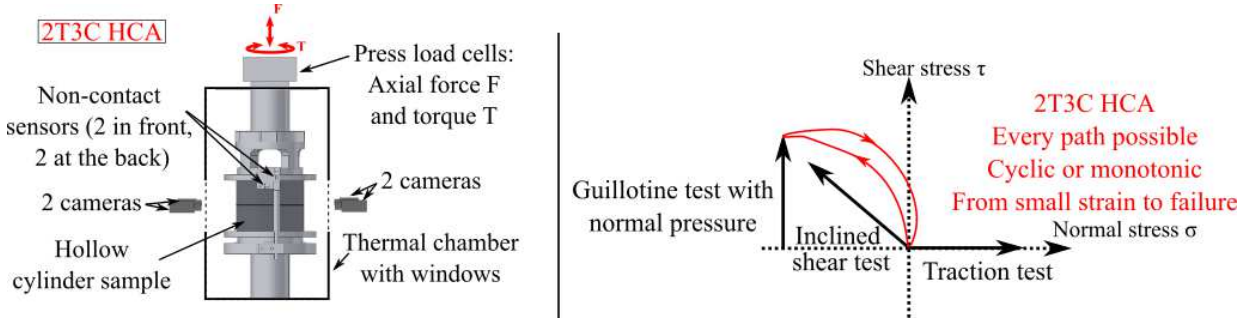


**Figure 2 - Scheme of the 2T3C HCA with measuring systems (left) and loading possibilities (right)**

The main innovation in the measuring systems of 2T3C HCA (Figure 2) is the use of 3D Digital Image Correlation (3D DIC) to observe the deformation at the interface. Only 2D DIC has already been used to study interfaces [11,15]. The 3D DIC computes the displacement in the three dimensions at the surface of the hollow cylinder by analysing pairs of pictures taken at different states of deformation during a test. The samples are painted with a random pattern to improve the 3D DIC precision. The displacements are computed on an area of 10 cm by 10 cm in the middle of the sample, centred on the interface. The subset size was fixed at 25 pixels after a parametric study, one pixel representing 150 µm of the material. A specific procedure developed at the ENTPE/University of Lyon is used to find the strain in the bituminous mixtures layers and the relative displacements, called displacement gaps, at the level of the interface. It is based on the calculation of averaged displacements on 24 horizontal strips (4 mm high) plotted in the bituminous mixtures layers on the pictures taken during the test. For the axial analysis (Figure 3), the displacement component along the vertical axis of the hollow cylinder, named $u_z$, is averaged on a strip and the average value is attributed to the centre of the strip with the vertical coordinate $Z$. In the layers, as the test is homogeneous, the slopes obtained in the $Z$-$u_z$ plot give access to the strain tensor components $\varepsilon_{zz}$ using linear regressions. The lines drawn in the layers do not intersect at the level of the interface. The relative displacement between the layers at the level of the interface is called vertical displacement gap $\Delta u_z$. A similar analysis adapted for the rotation displacement $u_\theta$ allows obtaining the strain tensor component $\varepsilon_{\theta z}$ in each layer and the rotation displacement gap $\Delta u_\theta$ at the interface. Another procedure gives access to $\varepsilon_{\theta\theta}$ [16].

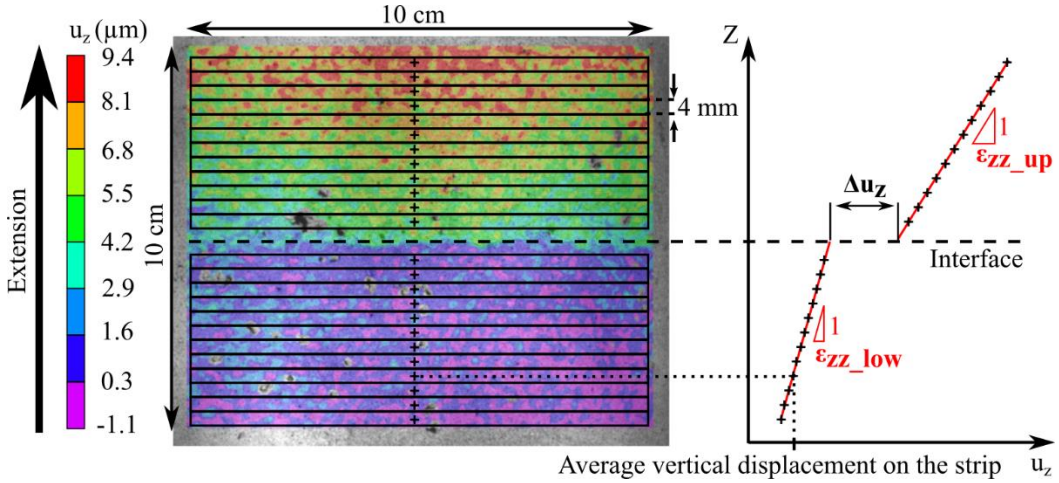


**Figure 3 - Vertical displacement $u_z$ from DIC averaged in each of the 24 strips of 10 cm x 4 mm and computation of $\varepsilon_{zz}$ in each asphalt layers and of the displacement gap $\Delta u_z$ at the interface (picture with a global extension of the sample of 12.5 µm)**

## 3. MATERIALS AND PROCEDURE

### 3.1. Tested materials

In this paper, the 2T3C HCA was used to perform a characterization of an interface between two bituminous mixtures with a tack coat in bituminous emulsion. A slab with two layers and a tack coat was made in laboratory. The first layer was made in the bituminous mixture EME2, used in France as a base course. It had a nominal maximum aggregate size (NMAS) of 14 mm, it contained 30 % of Reclaimed Asphalt Pavement (RAP) and a fresh bitumen with a 15/25 grade was used. The binder (including RAP bitumen) represented 5.6 % of the total mix weight. After 24 hours, the tack coat made of a bitumen emulsion of pure bitumen 160/220 was applied with a brush in order to have a residual bitumen dosage of 350 g/m². After another 24 hours, the emulsion had broken and the upper layer was laid. It was composed of a bituminous mixture BB5 employed in France as a surface course. It had a NMAS of 10 mm, 15 % of RAP and a total binder content of 5.1 % of the total mix weight. The fresh bitumen used was a modified bitumen with a 50/70 grade. Each layer was compacted with a wheel compactor, the void ratio was 1.0 % in the BB5 layer and 2.5 % in the EME2 layer. The slab was 600 mm long, 400 mm wide and 150 mm high, with the interface at mid-height.
Three hollow cylinders were cored in this slab and tested. They were named G6, D6 and M6. The coring was done first in the inside and then on the outside of the sample. The samples were then painted for the 3D DIC with a thin coat of white paint and sprayed black paint to get a random pattern at the surface. Finally, the samples were glued to aluminium caps at their extremities and ready to be instrumented and installed on the hydraulic press.

### 3.2. Advanced complex modulus test with 2T3C HCA

Each sample was tested first in the small strain domain and then up to failure. In the small strain domain, cyclic sinusoidal loadings were applied at several frequencies (0.01 Hz; 0.03 Hz; 0. 1 Hz; 0.3 Hz) and temperatures (10 °C; 20 °C; 30 °C; 40 °C) as presented in Figure 4. For each temperature, 5 rotation cycles at each frequency were applied with a slight and constant compression ($\sigma_{zz}$ = 15 kPa) and then 5 axial cycles at each frequency were applied with no shear stress ($\tau_{\theta z}$ = 0 MPa). The cycles amplitude was controlled using the non-contact sensors. The amplitude was chosen so that the global strain in a homogeneous sample of the same size would be 200 µm/m (the strain is $\varepsilon_{\theta z\_0}$ for rotation cycles and $\varepsilon_{zz\_0}$ for axial cycles). After the end of the test, the 3D DIC analysis was performed and the amplitude of the strain in the layer and the displacement gaps at the interface were found. They depend on the difference of behaviour between the lower layer, the upper layer and the interface which changes with the temperature and the frequency of the test. The vertical strain amplitudes $\varepsilon_{zz\_0}$ in the lower layer varied between 100 µm/m and 200 µm/m, and between 200 µm/m and 300 µm/m in the upper layer. The vertical displacement gap amplitudes $\Delta u_{z\_0}$ were between 1 µm and 2 µm. The shear strain amplitudes $\varepsilon_{\theta z\_0}$ in the lower layer varied between 100 µm/m and 200 µm/m, and between 200 µm/m and 300 µm/m in the upper layer. The horizontal displacement gap amplitudes $\Delta u_{\theta\_0}$ were between 4 µm and 8 µm.

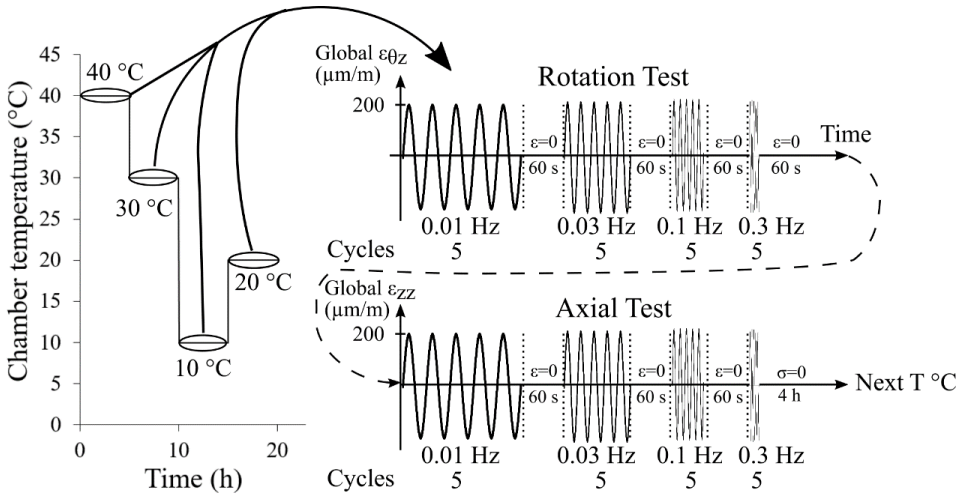


**Figure 4 - Advanced complex modulus test with the 2T3C HCA, test is controlled in displacement mode with an amplitude corresponding to 200 µm/m in global strain ($\varepsilon_{zz\_0}$ for axial tests or $\varepsilon_{\theta z\_0}$ for rotation tests) for a homogeneous material sample**

Using the cameras, 50 pictures were taken for each cycle for all frequencies at the exception of 0.3 Hz cycles where 30 pictures per cycle were taken. The stress measurements were acquired at the exact same time that pictures were

taken. An example of result is presented on Figure 5, one dot representing one set of pictures analysed with 3D DIC and the continuous lines being the least square approximations used for further analysis.

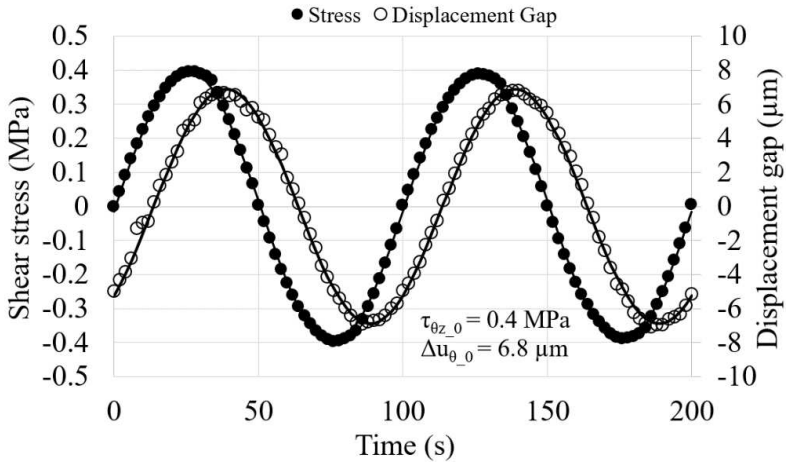


**Figure 5 - Example of stress and displacement gap measurements for the rotation test at f = ω/2π = 0.01 Hz and T = 10 °C on the sample G6 (BB5/EME2, 350 g/m² of tack coat) with least square approximations in continuous lines**

The normal complex interface stiffness $K_{zz}$* is defined in Equation (1) where $\sigma_{zz\_0}$ is the normal stress amplitude, $\Delta u_{z\_0}$ is the vertical displacement gap amplitude at the level of the interface and $\varphi_{Kzz}$ is the phase angle between the signals.

$$K_{zz}^{*} = \frac{\sigma_{zz\_0}}{\Delta u_{z\_0}} \; e^{i\varphi_{Kzz}} = |K_{zz}^{*}| e^{i\varphi_{Kzz}} \qquad (1)$$

The shear complex interface stiffness $K_{\theta z}$* is defined in Equation (2) where $\tau_{\theta z\_0}$ is the shear stress amplitude, $\Delta u_{\theta\_0}$ is the rotation displacement gap amplitude at the level of the interface and $\varphi_{K\theta z}$ is the phase angle between the signals.

$$K_{\theta z}^{*} = \frac{\tau_{\theta z\_0}}{\Delta u_{\theta\_0}} \; e^{i\varphi_{K\theta z}} = |K_{\theta z}^{*}| e^{i\varphi_{K\theta z}} \qquad (2)$$

### 3.3. Monotonic failure test

After the samples were tested in the small strain domain, they were subjected to a monotonic failure test. The samples were conditioned at the temperature of 18.5 °C during at least 4 h before the beginning of the test. A constant rotation of 0.033 °/s between the top and the bottom of the sample was imposed until the specimens failed. This represents a shear strain rate of 1 %/s at the level of the mean radius in a homogeneous material sample. Pictures are taken at a rate of 2 Hz for the 3D DIC analysis. During the twisting, the normal stress was maintained constant: at 0 MPa for sample G6, at 0.25 MPa for sample D6 (compression) and at 1 MPa (compression) for sample M6. The interface shear strength is defined as the maximum shear stress reached in the test. The vertical displacement gap and horizontal displacement gap during the rotation were obtained after the end of the test.

## 4. RESULTS AND DISCUSSION

### 4.1. Small strain behaviour

When plotting the isotherm curves of the norm of the complex interface stiffnesses versus the frequency, it was possible to shift the isotherms along the frequency axis in order to build a unique curve called the mastercurve for the norm of both the normal complex interface stiffness $|K_{zz}$*| (Figure 6) and the shear complex interface stiffness $|K_{\theta z}$*| (Figure 7). The mastercurves were plotted for a reference temperature of 15 °C.

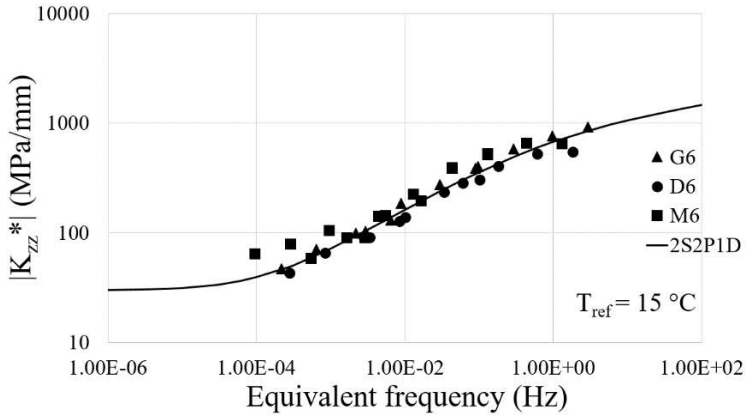


**Figure 6 - Mastercurves of normal complex interface stiffness norm $|K^*_{zz}|$ for the three samples (G6, D6, M6) at the reference temperature of 15 °C**

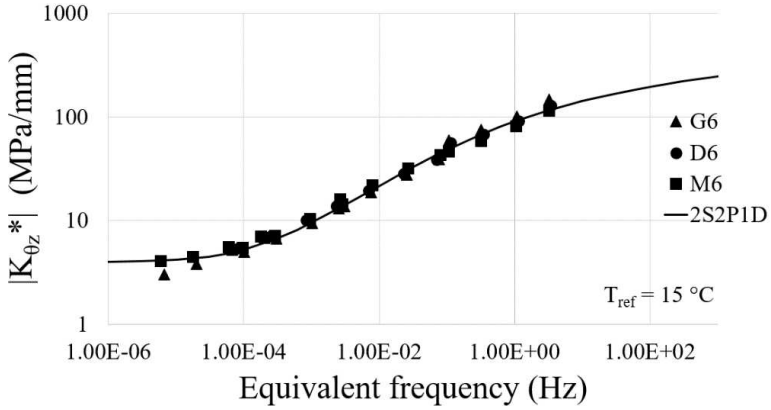


**Figure 7 - Mastercurves of shear complex interface stiffness norm $|K^*_{\theta z}|$ for the three samples (G6, D6, M6) at the reference temperature of 15 °C**

This indicates that the interface stiffness norm respects the Time-Temperature Superposition Principle (TTSP), meaning that the behaviour at high frequencies is equivalent to the behaviour at low temperatures (and the behaviour at low frequencies is the same as the one for high temperatures). A good repeatability was observed for the results of the three samples. The shift factors $a_T$ used to obtain the mastercurve are plotted against the temperature in Figure 8 for a reference temperature of 15 °C.

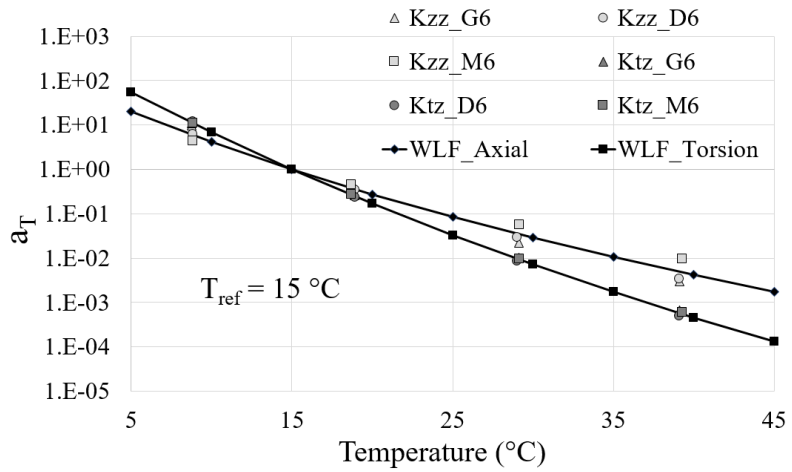


**Figure 8 – Shift factors with WLF equation for normal interface behaviour and shear interface behaviour**

On Figure 8 are also represented in continuous lines the WLF equations (Equation (3)) fitted on the shift factors data. The parameters of the WLF equation, $C_1$ and $C_2$, are presented in Table 1.

$$log(a_T) = \frac{-C_1(T - T_{ref})}{C_2 + T - T_{ref}} \quad (3)$$

The mastercurves of the norm of the interface modulus were modelled using the 2S2P1D model [17] presented in equation (4) where ω is the angular frequency, $K_0$ the static modulus, $K_{00}$ the glassy modulus, k, h, δ, β are calibration constants and τ is a characteristic relaxation time.

$$K^*_{2S2P1D}(\omega) = K_{00} + \frac{K_0 - K_{00}}{1 + \delta(i\omega\tau)^{-k} + (i\omega\tau)^{-h} + (i\omega\beta\tau)^{-1}} \quad (4)$$

The parameters of the models are presented in Table 1. One model was fitted for the axial behaviour of the three samples and one model for the shear behaviour of the three samples. The models were then plotted in Figure 6 and Figure 7.

**Table 1. 2S2P1D constants for interface behaviour at reference temperature 15 °C**

| | $K_{00}$ [MPa/mm] | $K_0$ [MPa/mm] | $k$ [-] | $h$ [-] | $\delta$ [-] | $\tau$ [s] | $\beta$ [-] | $C1$ [-] | $C2$ [°C] |
|---|---|---|---|---|---|---|---|---|---|
| Normal modulus | 30 | 3000 | 0.2 | 0.53 | 2.3 | 0.1 | 300 | 12.5 | 106.3 |
| Shear modulus | 4 | 400 | 0.2 | 0.53 | 2.3 | 0.1 | 300 | 19.9 | 124.1 |

### 4.2. Failure test

In the three tests performed at different normal pressures the failure always happened at the interface. Using the 3D DIC, the vertical and horizontal displacement gaps at the interface were obtained during the test. The evolution of the shear stress at the interface with the horizontal displacement gap is presented in Figure 9. The curves present a peak corresponding to the interface failure. The interface shear strength and the value of vertical and horizontal displacement gaps at failure are presented in Table 2. The displacement gaps after failure were not found because of DIC inability to measure large displacements with the setup of this study.

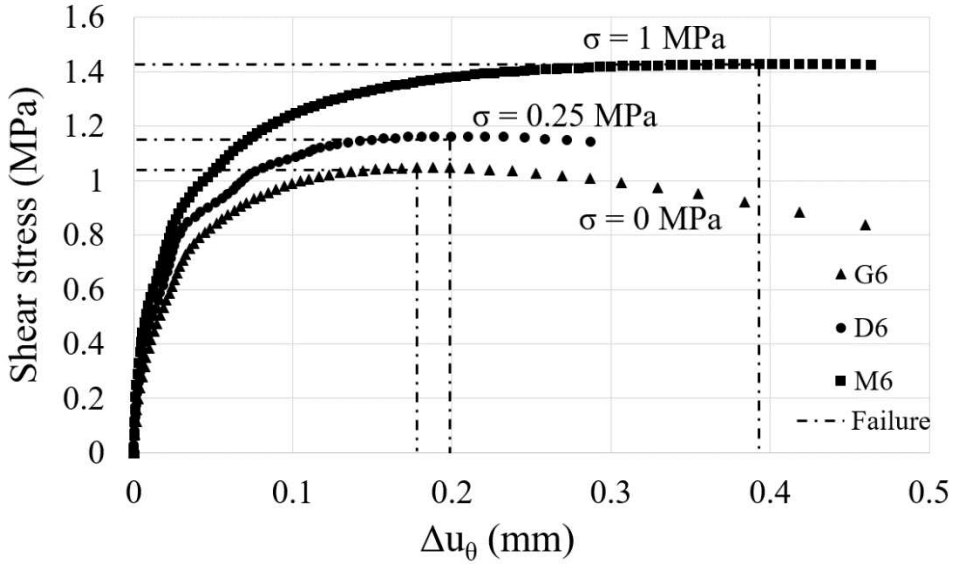


**Figure 9 – Shear stress $\tau$ evolution with the rotation displacement gap $\Delta u_\theta$ for the three failure tests at different normal stresses $\sigma$**

**Table 2. Failure tests results**

| Sample | Normal stress $\sigma$ [MPa] | Shear strength $\tau_{max}$ [MPa] | Rotation displacement gap at failure $\Delta u_{\theta\_max}$ [mm] | Vertical displacement gap at failure $\Delta u_{z\_max}$ [mm] |
|---|---|---|---|---|
| G6 | 0 | 1.05 | 0.178 | 0.037 |
| D6 | 0.25 | 1.16 | 0.199 | 0.038 |
| M6 | 1 | 1.43 | 0.394 | -0.057 |

When the normal pressure is increased, the shear strength of interfaces improves and the peak value is obtained for a higher horizontal displacement gap. The vertical displacement gap at failure is positive when the normal pressure is low meaning that space is created at the interface to allow the layer's horizontal relative displacement. But if the normal stress is too high ($\sigma$ = 1 MPa), the vertical displacement is negative and the interface is being compressed.

## 5. CONCLUSIONS

Using the innovative 2T3C Hollow Cylinder Apparatus, the thermomechanical behaviour of a laboratory made bi-layered material with two bituminous mixtures (BB5 and EME2) and a tack coat at the interface in pure bitumen emulsion was studied in the small strain domain and at failure. 3D Digital Image Correlation was used to find displacement gaps as low as 1 µm at the level of the interface.

In the small strain domain, cyclic testing was performed in tension/compression and in torsion. The normal complex interface stiffness $K_{zz}$* and the shear complex interface stiffness $K_{\theta z}$* were obtained for different temperatures and frequencies with a good repeatability. The interface behaviour respects the Time-Temperature Superposition Principle and the mastercurves were obtained. The norm of the complex interface stiffnesses was modelled using the 2S2P1D model.

Monotonic shear tests were performed until failure with a constant normal stress. Three samples of the studied material were tested, each sample with a different normal stress (0 MPa; 0.25 MPa; 1 MPa). The shear strength improves when the normal pressure increases and failure happens for larger horizontal displacement gaps when normal pressure is applied.

## ACKNOWLEDGEMENTS

This work is part of the industrial chair between ENTPE/University of Lyon and the company EIFFAGE dedicated to pavement materials and structures.

## REFERENCES

[1] AASHTO. *Guide for Design of Pavement Structure*. American Association of State Highway and Transportation. (2002)

[2] LCPC, and SETRA. *Conception et Dimensionnement Des Structures de Chaussée*. Ministère de l'Equipement, des Transports et du Tourisme. (1994)

[3] Burmister, D. M. "The General Theory of Stresses and Displacements in Layered Soil Systems. II." *Journal of Applied Physics* 16 (3) (1945) 126–27. https://doi.org/10.1063/1.1707562.

[4] Uzan, J., H. Livneh, and Y. Eshed. "Investigation of Adhesion Properties between Asphaltic-Concrete Layers." *Association of Asphalt Paving Technologists Proc* 47 (1978) 495–521.

[5] D'Andrea, Antonio, and Cristina Tozzo. "Interface Stress State in the Most Common Shear Tests." *Construction and Building Materials* 107 (March) (2016) 341–55. https://doi.org/10.1016/j.conbuildmat.2016.01.016.

[6] Di Benedetto, Hervé, and Jean-François Corté. *Matériaux routiers bitumeux 2: constitution et propriétés thermomécaniques des mélanges*. Paris: Hermès Science Publications. (2005)

[7] Leutner, R. "Untersuchung Des Schichtenverbundes Beim Bituminosen Oberbau" *Bitumen* 41 (3) (1979) 84–91.

[8] Raab, Christiane, and Manfred N. Partl. "Effect of Tack Coats on Interlayer Shear Bond of Pavements." In *Proceedings of the 8th Conference on Asphalt Pavements for Southern Africa (CAPSA'04)*, 12:16. (2004)

[9] Raposeiras, Aitor C., Ángel Vega-Zamanillo, Miguel Ángel Calzada-Pérez, and Daniel Castro-Fresno. "Influence of Surface Macro-Texture and Binder Dosage on the Adhesion between Bituminous Pavement Layers." *Construction and Building Materials* 28 (1) (2012) 187–92. https://doi.org/10.1016/j.conbuildmat.2011.08.029.

[10] Zofka, Adam, Maciej Maliszewski, Alexander Bernier, Ramandeep Josen, Audrius Vaitkus, and Rita Kleizienė. "Advanced Shear Tester for Evaluation of Asphalt Concrete under Constant Normal Stiffness Conditions." *Road Materials and Pavement Design* 16 (sup1) (2015) 187–210. https://doi.org/10.1080/14680629.2015.1029690.

[11] Cho, Seong Hwan, Seyed Amirshayan Safavizadeh, and Y. Richard Kim. "Verification of the Applicability of the Time–Temperature Superposition Principle to Interface Shear Stiffness and Strength of GlasGrid-Reinforced Asphalt Mixtures." *Road Materials and Pavement Design* 18 (4) (2017) 766–84 https://doi.org/10.1080/14680629.2016.1189350

[12] Canestrari, Francesco, Gilda Ferrotti, Manfred Partl, and Ezio Santagata. "Advanced Testing and Characterization of Interlayer Shear Resistance." *Transportation Research Record: Journal of the Transportation Research Board* 1929 (January) (2005) 69–78. https://doi.org/10.3141/1929-09.

[13] D'Andrea, Antonio, Cristina Tozzo, Alberto Boschetto, and Luana Bottini. "Interface Roughness Parameters and Shear Strength." *Modern Applied Science* 7 (10) (2013) https://doi.org/10.5539/mas.v7n10p1.

[14] Hight, D. W., A. Gens, and M. J. Symes. "The Development of a New Hollow Cylinder Apparatus for Investigating the Effects of Principal Stress Rotation in Soils." *Géotechnique* 33 (4) (1983) 355–83. https://doi.org/10.1680/geot.1983.33.4.355.

[15] Ktari, Rahma, Anne Millien, Fazia Fouchal, Ion-Octavian Pop, and Christophe Petit. "Pavement Interface Damage Behavior in Tension Monotonic Loading." *Construction and Building Materials* 106 (March) (2016) 430–42. https://doi.org/10.1016/j.conbuildmat.2015.12.020.

[16] Attia, Thomas, Hervé Di Benedetto, Cédric Sauzéat, François Olard, and Simon Pouget. "Hollow Cylinder Apparatus to Characterize Interfaces between Pavement Layers." *71st RILEM Annual Week & ICACMS Proceedings* (2017) 4:401–10. Chennai.

[17] Olard, François, and Hervé Di Benedetto. "General '2S2P1D' Model and Relation Between the Linear Viscoelastic Behaviours of Bituminous Binders and Mixes." *Road Materials and Pavement Design* 4 (2) (2003) 185–224. https://doi.org/10.1080/14680629.2003.9689946.